

Electronic Supplementary Information

**Coordinately Unsaturated Metal-Organic Framework as an Unpyrolyzed
Bifunctional Electrocatalyst for Oxygen Reduction and Evolution Reactions**

Hao Wang^{b,c}, Xiudu Zhang^d, Fengxiang Yin^{a,*}, Wenyu Chu^c, Biaohua Chen^{a,b}

^a *Jiangsu Key Laboratory of Advanced Catalytic Materials and Technology, School of Petrochemical Engineering, Changzhou University, Changzhou 213164, PR China.*

^b *College of Environmental and Energy Engineering, Beijing University of Technology, Beijing 100124, PR China.*

^c *College of Chemical Engineering, Beijing University of Chemical Technology, Beijing 100029, PR China.*

^d *State Key Laboratory of Coordination Chemistry, Nanjing University, Nanjing 210023, PR China.*

* Corresponding author

E-mail: yinfx@cczu.edu.cn (F. Yin)

S1 Experimental method

S1.1 Kinetics analysis

The kinetic-controlled process of ORR can be described by Tafel equation and mass-transport-corrected current densities were introduced as below:

$$\eta = \frac{2.3RT}{\alpha n_a F} \lg i^0 - \frac{2.3RT}{\alpha n_a F} \lg |i| \quad (\text{S1})$$

$$i_K = \frac{i_L \cdot i}{i_L - i} \quad (\text{S2})$$

where η is the overpotential; i^0 is the exchange current density; R is the universal gas constant; T is the temperature; α is the transfer coefficient; n_a is the mole number of electrons; and F is the Faraday constant i_K is the mass-transport corrected kinetic current density; i_L is the diffusion-limiting current density; and i is the apparent current density.

S1.2 Diffusion-limiting properties

The diffusion-controlled ORR process catalyzed by the samples can be analyzed by Koutechy-Levich (K-L) equation shown as follows:

$$\frac{1}{i} = \frac{1}{i_K} + \frac{1}{i_L} = \frac{1}{i_K} + \frac{1}{B\omega^{1/2}} \quad (\text{S3})$$

$$B = 0.62nFD_{O_2}^{2/3}\nu^{-1/6}C_0 \quad (\text{S4})$$

$$i_K = nFkC_0 \quad (\text{S5})$$

where ω is the angular velocity of the disk electrode, n is the overall number of electrons transferred in the O_2 reduction process, F is the Faraday constant, D_{O_2} is the diffusion coefficient of O_2 , C_0 is the saturated concentration of O_2 in 0.1 M KOH at 1 atm O_2 pressure, and ν is the kinematical viscosity of the electrolyte.

S1.3 Electron transfer number analysis

The Pt-ring electrode potential was fixed at 1.46 V and the glassy carbon-disk electrode was set to sweep from 1.00 to 0.20 V during the RRDE experiments at an electrode rotation rate of 1600 rpm. The collection efficiency (N), which was measured under a nitrogen atmosphere using 10 mM K₃[Fe(CN)₆], was observed to be 0.38. This value is very similar to the theoretical value of 0.37. Hydrogen peroxide yields and the electron transfer number (n) were calculated using the following equations:

$$HO_2^- (\%) = 200 \frac{I_r / N}{I_d + I_r / N} \quad (S6)$$

$$n = \frac{I_d}{I_d + I_r / N} \quad (S7)$$

where I_r is ring current; I_d is disk current.

S1.4 Electrochemical test to characterize the catalysts after CV cycling

The ground Co-BTC-IMI was pressed into a thin film, which was clipped as a working electrode. No ionomer or carbon black was added during the working electrode fabrication to avoid any interference of other elements. The reference electrode and the counter electrode remain the same as used for RDE experiments. The working electrode was subjected to 500 CV cycling at 50 mV·s⁻¹ in the potential range of 0.80 to 1.55 V vs. RHE in O₂-saturated 0.1 M KOH. After the cycling, the catalyst was collected and washed by water for multiple times to remove the electrolyte. After vacuum dry at 80 °C overnight, the catalyst was ready for XPS and BET studies to investigate its compositional and structural changes upon electrochemical reactions.

S2. Crystallographic structure of Co-BTC

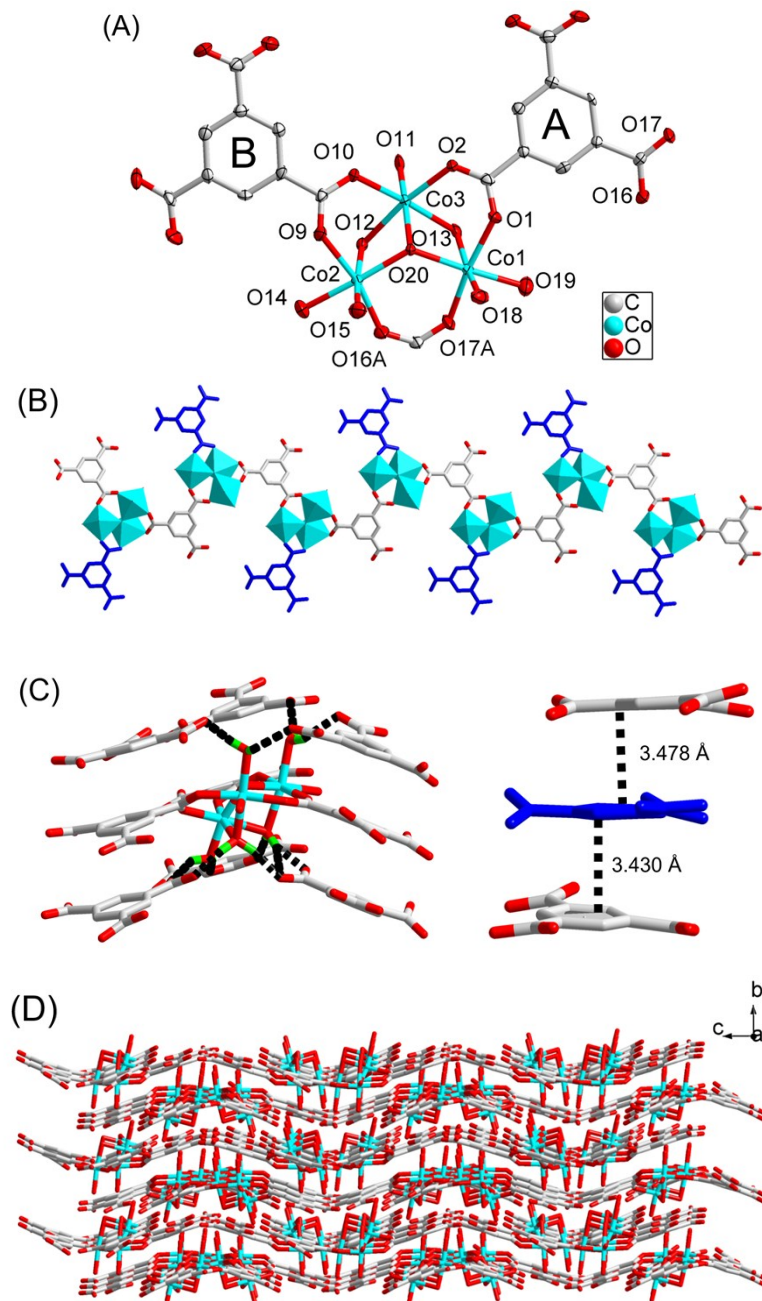


Fig. S1 (A) Coordination environment of Co(II) in Co-BTC with ellipsoids drawn at 50% probability level. The hydrogen atoms are omitted for clarity. Symmetry codes: A, -1/2+x, -y, 1/2-z. (B) The 1D coordination chains constructed from BTC³⁻ and Co²⁺ and the B-type ligands are depicted in blue. (C) The hydrogen bonding interactions involving between coordination water molecules and unbound carboxylate groups of BTC³⁻ and the π-π stacking interactions between BTC³⁻. (D) The final 3D supramolecular architecture of Co-BTC.

S3. Crystallographic parameters

Table S1. Crystal Data and Structure Refinements for Co-BTC-IMI and Co-BTC.

Compound	Co-BTC-IMI	Co-BTC
chemical formula	C ₂₄ H ₃₆ N ₄ O ₂₂ Co ₂	C ₁₈ H ₂₀ O ₂₀ Co ₃
formula weight	850.43	733.13
crystal system	Triclinic	Orthorhombic
space group	P-1	Pbca
<i>a</i> /Å	9.1263(12)	18.975(4)
<i>b</i> /Å	9.3577(13)	14.660(3)
<i>c</i> /Å	10.6375(14) 79.337(2)	21.497(4) 90
β /°	87.505(2) 71.929(2)	90 90
temperature /K	296(2) K	296(2)
volume /Å ³	848.6(2)	5980(2)
<i>Z</i>	1	8
D _c /g cm ⁻³	1.664	1.629
μ /mm ⁻¹	1.074	1.726
<i>F</i> (000)	438	2952
reflections collected / unique	6080 / 4203	30897 / 5269
GOF	1.077	1.048
<i>R</i> ₁ ,	R ₁ = 0.0310,	R ₁ = 0.0598,
<i>wR</i> ₂ [<i>I</i> > 2σ(<i>I</i>)] ^{a,b}	<i>wR</i> ₂ = 0.0984	<i>wR</i> ₂ = 0.1553
<i>R</i> ₁ ,	R1 = 0.0338,	R ₁ = 0.0815,
<i>wR</i> ₂ (all data)	<i>wR</i> 2 = 0.1004	<i>wR</i> ₂ = 0.1653

^a*R*₁ = Σ||*F*_o| - |*F*_c||/Σ|*F*_o|. ^b*wR*₂ = [Σ*w*(|*F*_o|² - |*F*_c|²)]/Σ|*w*(*F*_o)²|^{1/2}, where *w* = 1/[σ²(*F*_o)² + (*aP*)² + *bP*]. *P* = (*F*_o² + 2*F*_c²)/3

Table S2. Selected Bond Length (Å) and Angles (°) for Co-BTC-IMI and Co-BTC.

Co-BTC-IMI			
Co(1)-O(8)	2.0861(14)	Co(1)-O(2)	2.0866(11)
Co(1)-O(7)	2.0990(14)	Co(2)-O(11)	2.0589(12)
Co(2)-O(9)	2.1055(14)	Co(2)-O(10)	2.1167(12)
O(8)-Co(1)-O(8)#1	180.00(7)	O(8)-Co(1)-O(2)	90.11(5)
O(8)-Co(1)-O(2)#1	89.89(5)	O(2)-Co(1)-O(2)#1	180.000(1)
O(8)-Co(1)-O(7)#1	87.88(7)	O(8)#1-Co(1)-O(7)#1	92.12(7)
O(2)-Co(1)-O(7)#1	90.23(5)	O(2)#1-Co(1)-O(7)#1	89.77(5)
O(7)-Co(1)-O(7)#1	180.0	O(11)-Co(2)-O(11)#2	180.00(7)
O(11)#2-Co(2)-O(9)#2	87.87(6)	O(11)-Co(2)-O(9)#2	92.13(6)
O(9)-Co(2)-O(9)#2	180.0	O(11)#1-Co(2)-O(10)#2	90.20(5)
O(11)-Co(2)-O(10)#2	89.80(5)	O(9)#2-Co(2)-O(10)#2	93.14(5)
O(9)#2-Co(2)-O(10)#2	86.86(5)	O(10)-Co(2)-O(10)#2	180.00(7)
Co-BTC			
Co(1)-O(17)	2.033(4)	Co(1)-O(20)	2.046(3)
Co(1)-O(1)	2.048(4)	Co(1)-O(19)	2.093(4)
Co(1)-O(18)	2.135(5)	Co(1)-O(13)	2.238(4)
Co(2)-O(16)	2.021(4)	Co(2)-O(9)	2.032(4)
Co(2)-O(20)	2.040(4)	Co(2)-O(14)	2.099(4)
Co(2)-O(15)	2.150(5)	Co(2)-O(12)	2.241(4)
Co(3)-O(11)	1.999(4)	Co(3)-O(20)	2.020(4)
Co(3)-O(2)	2.093(4)	Co(3)-O(10)	2.099(4)
Co(3)-O(13)	2.246(4)	Co(3)-O(12)	2.246(4)
O(17)-Co(1)-O(20)	96.15(15)	O(17)-Co(1)-O(1)	170.96(17)
O(20)-Co(1)-O(1)	92.05(15)	O(17)-Co(1)-O(19)	84.52(17)
O(20)-Co(1)-O(19)	174.81(18)	O(1)-Co(1)-O(19)	86.97(17)
O(17)-Co(1)-O(18)	95.67(18)	O(20)-Co(1)-O(18)	93.19(16)
O(1)-Co(1)-O(18)	87.65(16)	O(19)-Co(1)-O(18)	91.86(19)
O(17)-Co(1)-O(13)	93.33(18)	O(20)-Co(1)-O(13)	83.86(14)
O(1)-Co(1)-O(13)	83.74(15)	O(19)-Co(1)-O(13)	90.96(17)
O(18)-Co(1)-O(13)	170.79(15)	O(16)-Co(2)-O(9)	166.20(17)
O(16)-Co(2)-O(20)	98.51(15)	O(9)-Co(2)-O(20)	94.80(14)
O(16)-Co(2)-O(14)	82.08(18)	O(9)-Co(2)-O(14)	84.35(17)
O(20)-Co(2)-O(14)	175.00(19)	O(16)-Co(2)-O(15)	88.43(18)
O(9)-Co(2)-O(15)	94.55(16)	O(20)-Co(2)-O(15)	92.88(16)

O(14) -Co(2)-O(15)	92.11(19)	O(16) -Co(2)-O(12)	93.91(17)
O(9) -Co(2)-O(12)	84.59(15)	O(20) -Co(2)-O(12)	80.85(14)
O(14) -Co(2)-O(12)	94.15(18)	O(15) -Co(2)-O(12)	173.57(15)
O(11) -Co(3)-O(20)	165.69(18)	O(11) -Co(3)-O(2)	92.80(17)
O(20) -Co(3)-O(2)	96.77(16)	O(11) -Co(3)-O(10)	92.62(17)
O(20) -Co(3)-O(10)	95.98(15)	O(2) -Co(3)-O(10)	100.88(15)
O(11) -Co(3)-O(13)	86.23(17)	O(20) -Co(3)-O(13)	84.24(14)
O(2) -Co(3)-O(13)	83.89(14)	O(10) -Co(3)-O(13)	175.16(15)
O(11) -Co(3)-O(12)	87.71(16)	O(20) -Co(3)-O(12)	81.17(14)
O(2) -Co(3)-O(12)	170.92(14)	O(10) -Co(3)-O(12)	88.15(14)
O(13) -Co(3)-O(12)	87.11(13)		

^a Symmetry transformations used to generate equivalent atoms: #1 -x, 1-y, 1-z; #2 1-x, 1-y, -z for Co-BTC-IMI.

Table S3. Hydrogen bonding data of Co-BTC-IMI and Co-BTC.

Co-BTC-IMI				
<i>D</i> -H···A	d(<i>D</i> -H) (Å)	d(H···A) (Å)	d(<i>D</i> ···A)(Å)	<i>D</i> -H···A (°)
N(1)-H(1)···O(6)	0.87	1.86	2.6952(4)	162
N(2)-H(2)···O(5)	0.89	1.89	2.7736(4)	174
O(7)-H(7A)···O(5)	0.91	1.94	2.8485(4)	173
O(8)-H(8A)···O(3)	0.91	2.09	2.9515(4)	158
O(8)-H(8B)···O(4)	0.95	1.78	2.7221(4)	173
O(9)-H(9A)···O(1)	0.95	1.73	2.6652(4)	167
O(9)-H(9B)···O(5)	0.90	1.85	2.7376(4)	166
O(10)-H(10B)···O(4)	0.84	1.87	2.7066(4)	172
O(10)-H(10C)···O(5)	0.90	2.00	2.8762(4)	163
O(11)-H(11B)···O(6)	0.88	1.84	2.7160(4)	174
O(11)-H(11C)···O(3)	0.87	1.84	2.7101(4)	175
C(11)-H(11A)···O(10)	0.93	2.53	3.4024(5)	157

Co-BTC				
O(11)-H(11A)···O(4)	0.85	1.92	2.5888(5)	134
O(11)-H(11B)···O(8)	0.85	1.80	2.6242(6)	164
O(12)-H(12A)···O(3)	0.97	1.74	2.6960(6)	168
O(12)-H(12B)···O(6)	0.97	1.73	2.6868(6)	167
O(13)-H(13A)···O(5)	0.97	1.74	2.6259(6)	149
O(13)-H(13B)···O(7)	0.97	1.88	2.7841(6)	155
O(15)-H(15A)···O(6)	0.85	2.39	3.0282(6)	133
O(15)-H(15C)···O(3)	0.85	2.12	2.7364(6)	129
O(18)-H(18A)···O(7)	0.85	2.01	2.7728(6)	148
O(18)-H(18B)···O(5)	0.85	2.01	2.7710(6)	149

Table S4. Comparison between the coordination information of Co(II) atoms in Co-BTC-IMI and Co-BTC

		Coordination number	Numbers of coordinated H ₂ O	Co-O _{carboxylate} (Å)	Co-O _{water} (Å)
Co-BTC-IMI	Co1	6	4	2.0866(11)	2.0861(14), 2.0990(14)
	Co2		6	--	2.0589(12) - 2.1167(12)
Co-BTC	Co1	6	4	2.033(4), 2.048(4)	2.046(3) - 2.238(4)
	Co2		4	2.021(4), 2.032(4)	2.040(4) - 2.241(4)
	Co3		4	2.093(4), 2.099(4)	1.999(4) - 2.246(4)
Co-BTC-IMI					
	D-H···A	d(D-H) (Å)	d(H···A) (Å)	d(D···A)(Å)	D-H···A (°)
	N(1)-H(1)···O(6)	0.87	1.86	2.6952(4)	162
	N(2)-H(2)···O(5)	0.89	1.89	2.7736(4)	174
	O(7)-H(7A)···O(5)	0.91	1.94	2.8485(4)	173
	O(8)-H(8A)···O(3)	0.91	2.09	2.9515(4)	158
	O(8)-H(8B)···O(4)	0.95	1.78	2.7221(4)	173
	O(9)-H(9A)···O(1)	0.95	1.73	2.6652(4)	167
	O(9)-H(9B)···O(5)	0.90	1.85	2.7376(4)	166
	O(10)-H(10B)···O(4)	0.84	1.87	2.7066(4)	172
	O(10)-H(10C)···O(5)	0.90	2.00	2.8762(4)	163
	O(11)-H(11B)···O(6)	0.88	1.84	2.7160(4)	174
	O(11)-H(11C)···O(3)	0.87	1.84	2.7101(4)	175
	C(11)-H(11A)···O(10)	0.93	2.53	3.4024(5)	157
Co-BTC					
	O(11)-H(11A)···O(4)	0.85	1.92	2.5888(5)	134
	O(11)-H(11B)···O(8)	0.85	1.80	2.6242(6)	164
	O(12)-H(12A)···O(3)	0.97	1.74	2.6960(6)	168
	O(12)-H(12B)···O(6)	0.97	1.73	2.6868(6)	167
	O(13)-H(13A)···O(5)	0.97	1.74	2.6259(6)	149
	O(13)-H13A···O(6)	0.97	2.52	3.3979(7)	151
	O(13)-H(13B)···O(7)	0.97	1.88	2.7841(6)	155
	O(15)-H(15A)···O(6)	0.85	2.39	3.0282(6)	133
	O(15)-H(15C)···O(3)	0.85	2.12	2.7364(6)	129
	O(18)-H(18A)···O(7)	0.85	2.01	2.7728(6)	148
	O(18)-H(18B)···O(5)	0.85	2.01	2.7710(6)	149

Table S5. Comparison of the π - π interactions between Co-BTC-IMI and Co-BTC

		d_{cent}	d_{perp}	d_{slip}
Co-BTC-IMI	BTC-BTC	3.6749(5)	3.3537	1.503
	BTC-IMI	3.6880(5)	3.3950	1.155
	IMI-IMI	4.2425(6)	3.4374	2.487
	C=O-IMI	3.8656(5)	3.560	--
Co-BTC	BTC-BTC	3.5914(8)	3.3743	1.160
		3.8046(8)	3.4453	1.426

d_{cent} : Distance between ring Centroids (Ang.).

d_{perp} : Perpendicular distance of ring A on ring B (Ang.).

d_{slip} : Distance between Cg(I) and Perpendicular Projection of Cg(J) on Ring I (Ang.).

Table S6. Comparison of the hydrogen bonds between Co-BTC-IMI and Co-BTC

		N-H \cdots O	O-H \cdots O	C-H \cdots O
Co-BTC-IMI	Numbers	2	9	1
	Range of lengths	2.6952(4), 2.7736(4)	2.6652(4) - 2.9515(4)	3.4024(5)
	Mid-value	--	2.7221(4)	--
Co-BTC	Numbers	--	11	--
	Range of lengths	--	2.5888(5) - 3.3979(7)	--
	Mid-value	--	2.7364(6)	--

S3. XPS full spectra of Co-BTC and Co-IMI

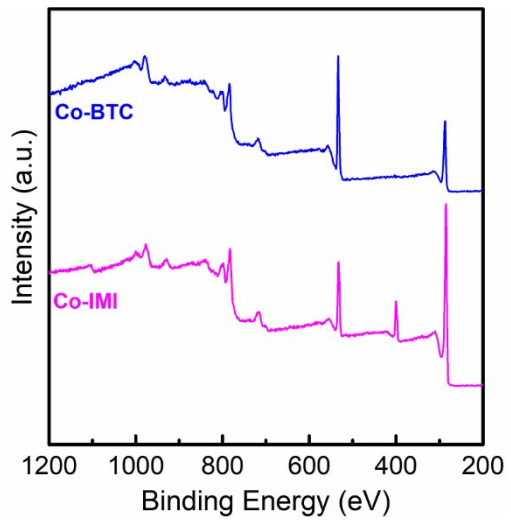


Fig. S2 XPS full spectra of Co-BTC and Co-IMI.

S4. K-L and electron transfer number analyses of Co-BTC-IMI

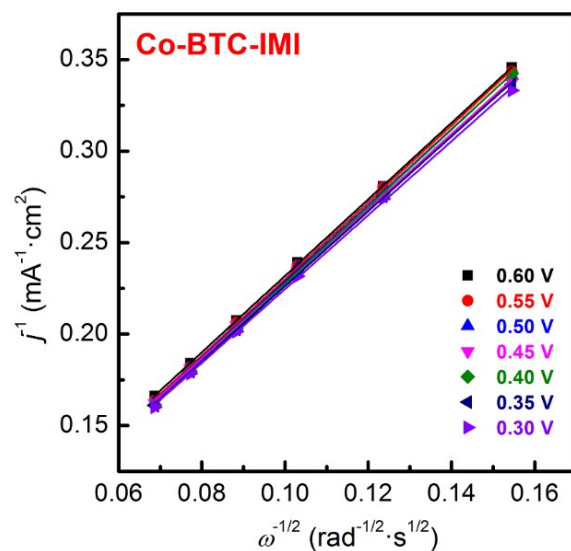


Fig. S3 K-L curves at various potentials for Co-BTC-IMI.

S5. RDE voltammograms and K-L curves for Co-BTC and Co-IMI

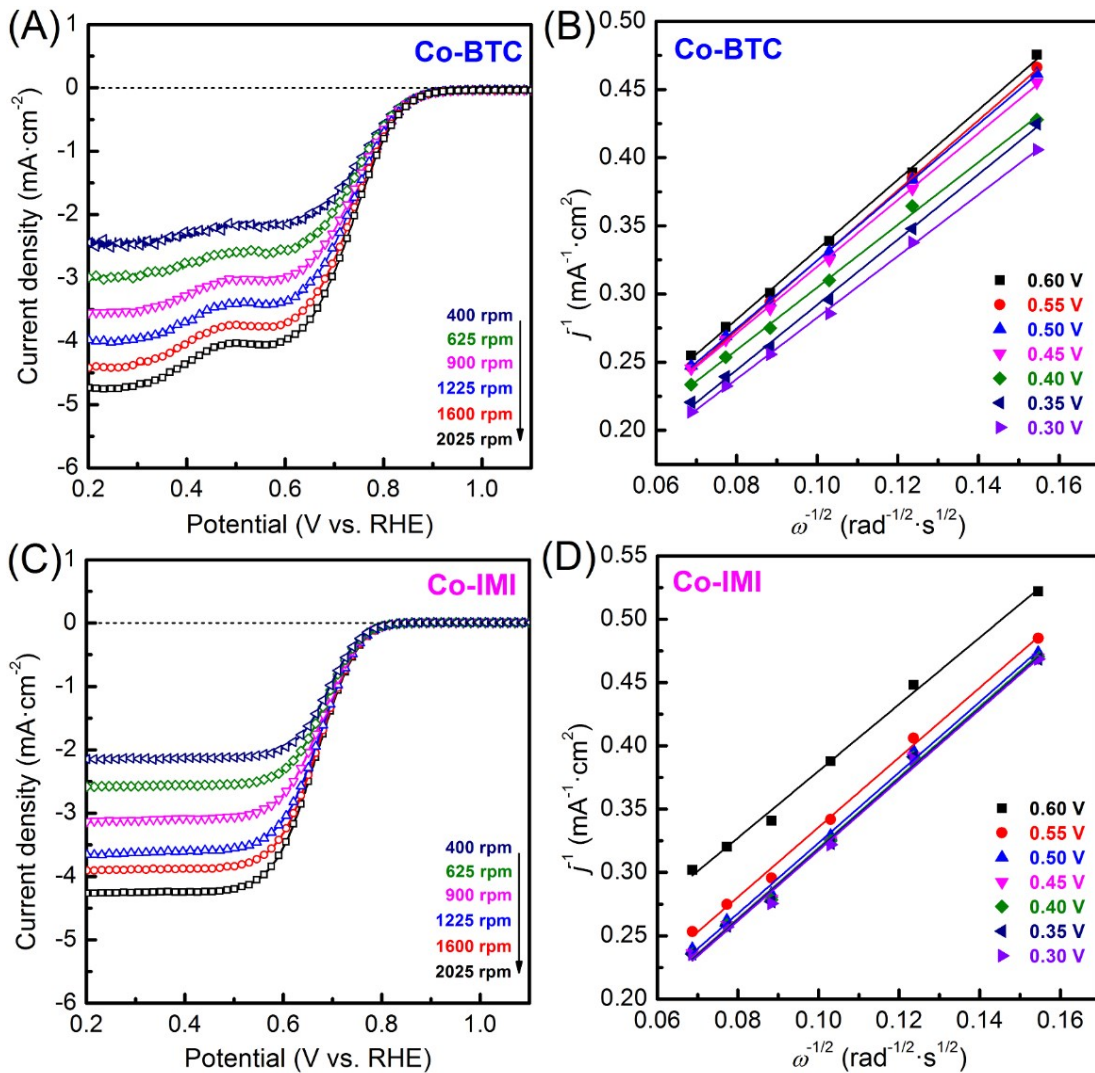


Fig. S4 ORR RDE voltammograms of (A) Co-BTC and (C) Co-IMI at different rotational speeds and (B, D) their corresponding K-L curves at different potentials.

S6. Electron transfer number derived from K-L curves for the studied MOFs

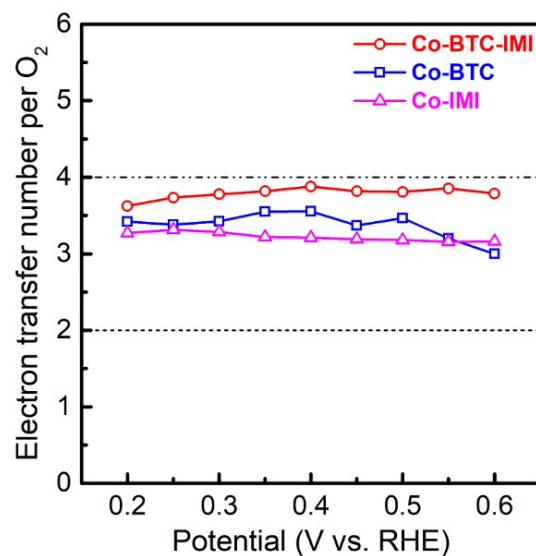


Fig. S5 Electron transfer number derived from the K-L curves for the studied MOFs.

S7. Modelling simulation details



Fig. S6 Simplified active site structures with the adsorbed intermediates during the electrocatalytic reaction process.

Table S7. The free energy difference of each reaction step during ORR over Co-BTC-IMI

ΔG of each step (eV)	U = 0 V	U = -0.83 V	U = -0.4 V	U = 0.4 V	U = 0.2 V
$\Delta G1$	-1.14	-1.14	-1.14	-1.14	-1.14
$\Delta G2$	0.11	-0.72	-0.29	0.51	0.31
$\Delta G3$	-5.87	-6.70	-6.27	-5.47	-5.67
$\Delta G4$	-0.56	-0.56	-0.56	-0.56	-0.56
$\Delta G5$	0.85	0.02	0.45	1.25	1.05

Table S8. The free energy difference of each reaction step during ORR over Co-BTC

ΔG of each step (eV)	U = 0 V	U = -0.83 V	U = -0.4 V	U = 0.4 V	U = 0.2 V
$\Delta G1$	-2.30	-2.30	-2.30	-2.30	-2.30
$\Delta G2$	1.63	0.80	1.23	2.03	1.83
$\Delta G3$	-6.07	-6.90	-6.47	-5.67	-5.87
$\Delta G4$	-0.46	-0.46	-0.46	-0.46	-0.46
$\Delta G5$	0.69	-0.14	0.29	1.09	0.89

S8. X-ray characterizations of Co-BTC-IMI before and after cycling

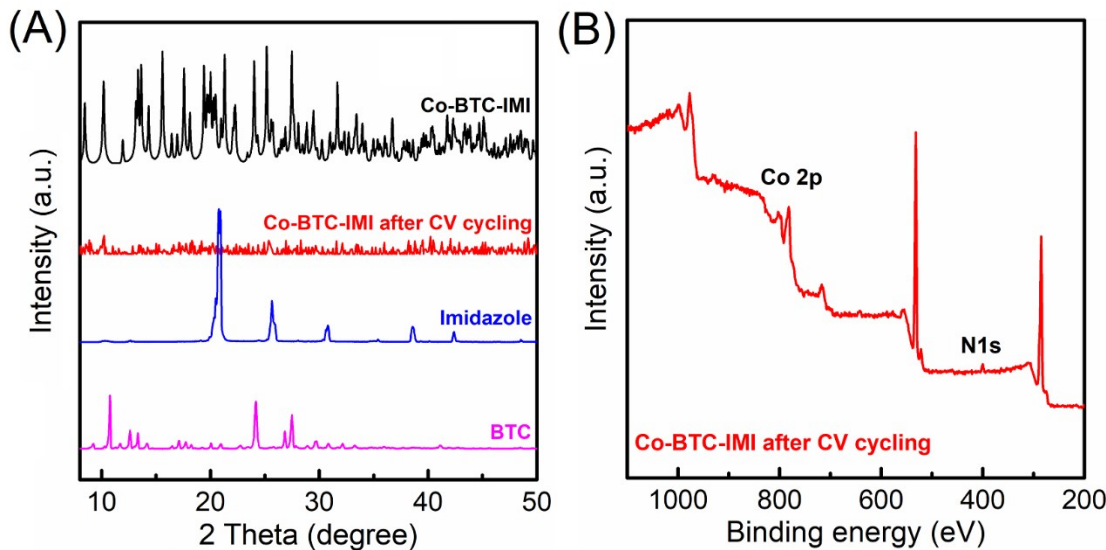


Fig. S7 (A) Powder XRD patterns of Co-BTC-IMI before and after CV cycling, imidazole and BTC. (B) XPS full spectrum of Co-BTC-IMI after CV cycling.

Table S9. Atomic percentage (at%) of the elements in Co-BTC-IMI

Samples	C 1s	O 1s	N 1s	Co 2p
Co-BTC-IMI before CV cycling	60.11	31.00	3.13	5.76
Co-BTC-IMI after CV cycling	66.01	29.27	1.68	3.04

S9. N₂ adsorption-desorption isotherms of Co-BTC-IMI before and after cycling

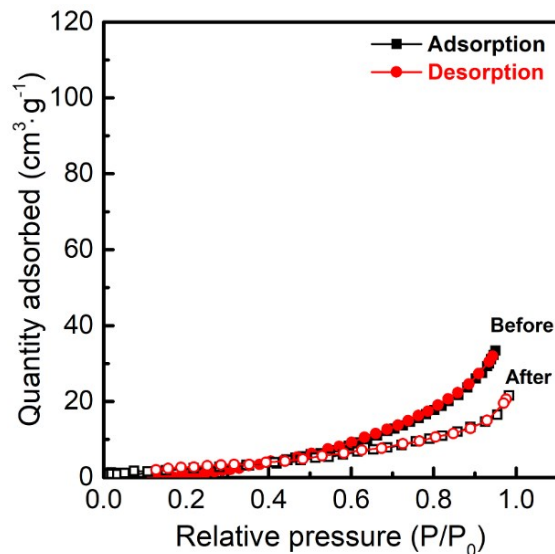


Fig. S8 N₂ adsorption-desorption isotherms of Co-BTC-IMI before and after cycling.

Table S10. BET specific surface area (SSA) of Co-BTC-IMI

Samples	BET SSA (m ² ·g ⁻¹)
Co-BTC-IMI before CV cycling	32.8
Co-BTC-IMI after CV cycling	19.6

S10. Bifunctional catalytic activity comparison

Table S11. ORR and/or OER activity comparison between Co-BTC-IMI and other unpyrolyzed MOFs reported in the literatures in 0.1M KOH by using RDE at 1600rpm

Catalyst	$E_{1/2, \text{ORR}}$ (V vs. RHE)	$E_{@j=10, \text{OER}}$ (V vs. RHE)	$\Delta E(E_{\text{OER}} - E_{\text{ORR}})$ (V vs. RHE)	Ref.
Co-BTC-IMI	0.80	1.59	0.79	This work
(G-dye 50 wt % -FeP) _n MOF	~0.46	--	--	S1
MOF(Fe)	~0.454	--	--	S2
MOF(Fe/Co)	~0.25	--	--	S3
α -MnO ₂ /MIL-101(Cr)	0.58	1.70	1.12	S4
ε -MnO ₂ /MOF(Fe)	0.64	--	--	S5
Co/MIL-101(Cr)-O	0.54	1.70	1.16	S6
nano-CuS(28 wt%)@Cu-BTC	~0.70	--	--	S7
Ni ₃ (HITP) ₂	~0.68	--	--	S8
Bulk NiCo-MOFs	--	1.55	--	S9
Fe/Ni-BTC@Ni foam	--	1.50	--	S10
Co-OBA/C	0.67	1.73	1.06	S11
ZIF-67@NPC	0.82	1.64	0.82	S12
NiFe-MOF	--	1.60	--	S13
Ti ₃ C ₂ T _x -Co-BDC	--	1.64	--	S14
Mn-BTC@AC	0.79	--	--	S15
FeCo-MNS-1.0	--	1.528	--	S16
PcCu-O8 - Co/CNT	0.83	--	--	S17
Co-MOF	0.55	1.51	0.96	S18

“~” in the following table indicates that the values were estimated directly from the figures

References

- S1. M. Jahan, Q. Bao and K. P. Loh, *Journal of the American Chemical Society*, 2012, **134**, 6707-6713.
- S2. G. Song, Z. Wang, L. Wang, G. Li, M. Huang and F. Yin, *Chinese Journal of Catalysis*, 2014, **35**, 185-195.
- S3. H. Wang, F. Yin, G. Li, B. Chen and Z. Wang, *International Journal of Hydrogen Energy*, 2014, **39**, 16179-16186.
- S4. F. Yin, G. Li and H. Wang, *Catalysis Communications*, 2014, **54**, 17-21.
- S5. H. Wang, F. Yin, B. Chen and G. Li, *Journal of Materials Chemistry A*, 2015, **3**, 16168-16176.
- S6. X. He, F. Yin and G. Li, *International Journal of Hydrogen Energy*, 2015, **40**, 9713-9722.
- S7. K. Cho, S. H. Han and M. P. Suh, *Angewandte Chemie International Edition*, 2016, **55**, 15301-15305.
- S8. E. M. Miner, T. Fukushima, D. Sheberla, L. Sun, Y. Surendranath and M. Dincă, *Nature Communications*, 2016, **7**, 1-7.
- S9. S. Zhao, Y. Wang, J. Dong, C.-T. He, H. Yin, P. An, K. Zhao, X. Zhang, C. Gao, L. Zhang, J. Lv, J. Wang, J. Zhang, A. M. Khattak, N. A. Khan, Z. Wei, J. Zhang, S. Liu, H. Zhao and Z. Tang, *Nature Energy*, 2016, **1**, 1-10.
- S10. L. Wang, Y. Wu, R. Cao, L. Ren, M. Chen, X. Feng, J. Zhou and B. Wang, *ACS Applied Materials & Interfaces*, 2016, **8**, 16736-16743.
- S11. T. Fan, F. Yin, H. Wang, X. He and G. Li, *International Journal of Hydrogen Energy*, 2017, **42**, 17376-17385.
- S12. H. Wang, F.-X. Yin, B.-H. Chen, X.-B. He, P.-L. Lv, C.-Y. Ye and D.-J. Liu, *Applied Catalysis B: Environmental*, 2017, **205**, 55-67.
- S13. J. Duan, S. Chen and C. Zhao, *Nature Communications*, 2017, **8**, 1-7.
- S14. L. Zhao, B. Dong, S. Li, L. Zhou, L. Lai, Z. Wang, S. Zhao, M. Han, K. Gao, M. Lu, X. Xie, B. Chen, Z. Liu, X. Wang, H. Zhang, H. Li, J. Liu, H. Zhang, X. Huang and W. Huang, *ACS Nano*, 2017, **11**, 5800-5807.
- S15. S. Gonen, O. Lori, G. Cohen-Taguri and L. Elbaz, *Nanoscale*, 2018, **10**, 9634-9641.
- S16. L. Zhuang, L. Ge, H. Liu, Z. Jiang, Y. Jia, Z. Li, D. Yang, R. K. Hocking, M. Li, L. Zhang, X. Wang, X. Yao and Z. Zhu, *Angewandte Chemie International Edition*, 2019, **131**, 13699-13706.
- S17. H. Zhong, K. H. Ly, M. Wang, Y. Krupskaya, X. Han, J. Zhang, J. Zhang, V. Kataev, B. Büchner, I. M. Weidinger, S. Kaskel, P. Liu, M. Chen, R. Dong and X. Feng, *Angewandte Chemie International Edition*, 2019, **131**, 10787-10792.
- S18. R. K. Tripathy, A. K. Samantara and J. Behera, *Dalton Transactions*, 2019, **48**, 10557-10564.